BIOCHEMISTRY
including biophysical chemistry & molecular biology

Article

pubs.acs.org/biochemistry

Phospholipid Bicelles Improve the Conformational Stability of Rhodopsin Mutants Associated with Retinitis Pigmentosa

Xiaoyun Dong, Eva Ramon, María Guadalupe Herrera-Hernández,[†] and Pere Garriga*

Grup de Biotecnologia Molecular i Industrial, Centre de Biotecnologia Molecular, Departament d'Enginyeria Química, Universitat Politècnica de Catalunya, Edifici Gaia, Rambla de Sant Nebridi 22, 08222 Terrassa, Catalonia, Spain

ABSTRACT: Mutations in the visual photoreceptor rhodopsin are the cause of the retinal degenerative disease retinitis pigmentosa. Some naturally occurring mutations can lead to protein conformational instability. Two such mutations, N55K and G90V, in the first and second transmembrane helices of the receptor, have been associated with sector and classical retinitis pigmentosa, respectively, and showed enhanced thermal sensitivity. We have carefully analyzed the effect of phospholipid bicelles on the stability and ligand binding properties of these two mutants and compared it with those of the detergent-solubilized samples. We have used a phospholipid bilayer consisting of 1,2-dimyristoyl-*sn*-glycero-3-phosphatidylcholine (DMPC) and 1,2-dihexanoyl-*sn*-glycero-3-phosphocholine (DHPC). We find that DMPC/DHPC bicelles dramatically increase the thermal stability of the rhodopsin mutants G90V and N55K. The chromophore stability and regeneration of the mutants were also increased in bicelles when compared to their behavior in a dodecyl maltoside detergent solution. The retinal release process was slowed in bicelles, and chromophore entry, after illumination, was improved for the G90V mutant but not for N55K. Furthermore, fluorescence spectroscopy measurements showed that bicelles allowed more exogenous retinal binding to the photoactivated G90V mutant than in a detergent solution. In contrast, N55K could not reposition any chromophore either in the detergent or in bicelles. The results demonstrate that DMPC/DHPC bicelles can counteract the destabilizing effect of the disease-causing mutations and can modulate the structural changes in the ensuing receptor photoactivation in a distinct specific manner for different retinitis pigmentosa mutant phenotypes.

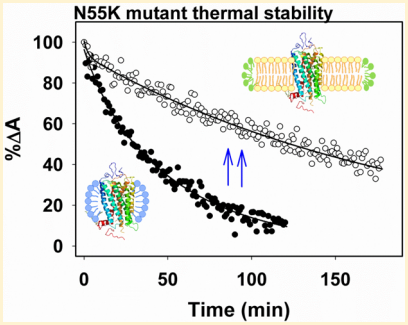

The visual photoreceptor rhodopsin (Rho) is a prototypical member of the G-protein-coupled receptor (GPCR) superfamily responsible for scotopic (or dim-light) vision. As a model of GPCRs, Rho has been extensively studied, and since the first report of its crystal structure, several GPCR structures have been determined by X-ray crystallography.[1−5] Rho is found in the rod outer segment (ROS) membranes of the photoreceptor cells of the retina where it is embedded in the lipid bilayer surrounded by ∼65−70 phospholipids per protein molecule.[6−9] Rho consists of the opsin apoprotein and the 11-*cis*-retinal ligand that is covalently bound through a protonated Schiff base (SB) linkage to K296 at the seventh transmembrane helix of the photoreceptor.[10−12] Upon photon absorption, the 11-*cis*-retinal chromophore isomerizes to all-*trans*-retinal and triggers a conformational change in the receptor that leads to the active metarhodopsin II (MetaII) photointermediate that can bind and activate the G-protein transducin.[11,13] Mutations in Rho are one of the main causes of retinitis pigmentosa (RP), which is a genetically heterogeneous disorder involving rod photoreceptor cell death and eventually leading to blindness.[14] The worldwide prevalence of RP is about 1 in 4000.[10,15] Misfolding and misassembly of mutant Rho, associated with RP, alter the cellular fate and induce cell death.[16,17] Some mutations alter the trafficking ability from the endoplasmic reticulum to the plasma membrane.[18] Sector retinitis pigmentosa (sector RP) is an atypical variant of RP. In sector RP, only isolated areas of the fundus show pigmentary changes. It is characterized by regionalized areas of bone spicule pigmentation usually found in the inferior quadrants of the retina, abnormal electro-retinograms, visual-field defects, and slow to no degeneration.[19]

Structure−function studies of Rho are typically conducted in the mild dodecyl maltoside (DM) detergent solution.[20,21] However, membrane proteins often show poor conformational stability and can lose activity or even be denatured in detergent micelles.[22,23] Membranelike environments help to maintain the proper structure and biochemical function of membrane proteins and their mutants.[24,25] Phospholipid bicelles have been shown to improve the stability of Rho,[26−28] and for this reason, we have studied two Rho mutants, G90V and N55K, and compared their properties in DM detergent and in DMPC/DHPC bicelles (Figure 1). G90V (causing the RP phenotype) and N55K (associated with sector RP) show structural instability in the dark and thermal sensitivity.[21,29,30] 9-*cis*-Retinal was used as an exogenous analogue[31,32] for a detailed characterization of these two specific Rho mutants. The thermal stability and chromophore regeneration ability of G90V and N55K improved in DMPC/DHPC bicelles, which provided a suitable bilayer environment for the mutants. MetaII decay experiments with the G90V mutant in bicelles showed an

Received: April 22, 2015
Revised: July 16, 2015
Published: July 16, 2015

DOI: 10.1021/acs.biochem.5b00435
Biochemistry 2015, 54, 4795−4804

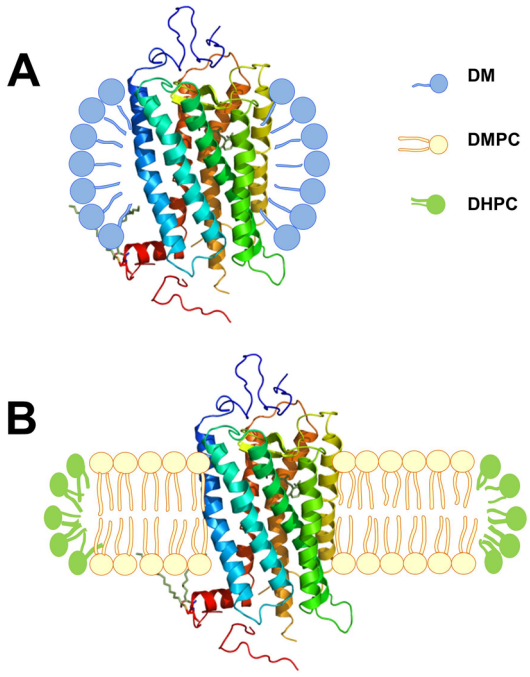

Figure 1. Schematic models for Rho in DM micelles and in DMPC/DHPC bicelles. (A) Schematic model for DM micelles with Rho. The hydrophobic tail of DM can wrap the hydrophobic transmembrane domain of the protein that is embedded in the core of the micelle. (B) Schematic model of DMPC/DHPC bicelles with embedded Rho. DMPC and DHPC form a bilayer structure.

additional fluorescence increase upon addition of hydroxylamine after complete retinal release but not for the N55K mutant. This suggested conformational differences in the photoactivated receptors affecting retinal accessibility to the postbleached opsin retinal binding pocket. Furthermore, the photoactived opsin conformation of the G90V RP mutant would be more efficient in allowing retinal to enter into the opsin binding pocket when the protein is in DMPC/DHPC bicelles than when it is in a DM detergent solution. In contrast, N55K opsin, in DMPC/DHPC bicelles, did not allow any chromophore to enter the opsin binding pocket. Overall, the results obtained indicate that DMPC/DHPC bicelles offer a stable bilayer environment for mutants associated with RP, but specific conformational differences can be observed for the two mutants, especially after photoactivation, which could be related to their different clinical phenotypes.

EXPERIMENTAL PROCEDURES

Materials. Rho was purified from bovine retinas, which were obtained from J. A. Lawson (Lincoln, NE). WT, G90V, and N55K opsin genes were cloned into the pMT4 vector. The chromophore 11-*cis*-retinal was provided by R. Crouch (National Eye Institute, National Institutes of Health, Bethesda, MD). 9-*cis*-Retinal was purchased from Sigma-Aldrich (St. Louis, MO). 1,2-Dimyristoyl-*sn*-glycero-3-phosphocholine [DMPC(14:0)] and 1,2-dihexanoyl-*sn*-glycero-3-phosphocholine [DHPC(6:0)] were purchased from Avanti Polar Lipids Inc. (Alabaster, AL), and *n*-dodecyl D-maltoside (DM) was from Anatrace (Maumee, OH).

Purified mAb rho-1D4 was provided by Cell Essentials (Boston, MA) and was coupled to CNBr-activated Sepharose 4B Fast Flow following the manufacturer's instructions (Amersham Biosciences). Secondary antibody goat anti-mouse IgG–HRP conjugate was purchased from Santa Cruz Biotechnology (Heidelberg, Germany). The 1D4 9-mer peptide corresponding to the last nine amino acids of Rho (TETSQVAPA) was synthesized by Serveis Cientificotècnics (Universitat de Barcelona, Barcelona, Spain). Hydroxylamine, protease inhibitor cocktail, phenylmethanesulfonyl fluoride (PMSF), and bis-tris-propane (BTP) were from Sigma-Aldrich (St. Louis, MO). Polyethylenimine 25 kDa (PEI) was purchased from Polysciences (Warrington, PA).

Buffers. The following buffers were used: buffer A consisting of 10 mM bis-tris-propane (BTP), 140 mM NaCl, 2 mM $MgCl_2$, and 2 mM $CaCl_2$ (pH 6.0) DM buffer consisting of buffer A containing 0.05% (w/v) DM, bicelle buffer consisting of buffer A containing 2% (w/v) DMPC/DHPC bicelles, and solvent buffer consisting of 137 mM NaCl, 2.7 mM KCl, 1.5 mM KH_2PO_4, and 8 mM Na_2HPO_4 (pH 7.4).

Cell Culture Materials. COS-1 cells were obtained from the American Type Culture Collection (Manassas, VA). DMEM, serum, and antibiotics were from Sigma-Aldrich. OPTIMEM reduced serum medium was from Life Technologies (Madrid, Spain).

Preparation of Bicelles. A 10% (w/v) DMPC sample was prepared by dissolving the powder in buffer A and gently vortexing, followed by incubating the solution at 42 °C for 5 min and then cooling to room temperature; 10% (w/v) DHPC was also prepared in buffer A. Final 2% (w/v) DMPC/DHPC (1:1) mixtures were mixed briefly, heated to 42 °C for 10 min, and then left to stir at room temperature for 1 h until the mixtures were clear (bicelle buffer). All bicelle solutions were used within 36 h of preparation.[26]

Expression, Purification, and Preparation of Rho, Recombinant WT, and Mutants. Rho refers to native Rho purified from bovine retinas, whereas WT refers to recombinant Rho heterologously expressed in COS-1 cells, immunopurified, and regenerated with 9-*cis*-retinal.

Rho Purification. ROS membranes were purified from bovine retinas using a sucrose gradient method under dim red light. The membranes were suspended in 70 mM potassium phosphate, 1 mM $MgCl_2$, and 0.1 mM EDTA (pH 6.9) and then subsequently centrifuged, and the pellets were resuspended in 5 mM Tris-HCl (pH 7.5) containing 0.5 mM $MgCl_2$. Two alternating washes with these buffers were conducted to remove any further contaminating proteins. Finally, ROS membranes were split into several aliquots and stored in the dark at −20 °C. The ROS membranes were used for Rho purification. ROS membranes were solubilized in solvent buffer with 1% (w/v) DM in the dark for 1 h at 4 °C. Then the sample was centrifuged at 35000 rpm (50 Ti rotor) for 30 min at 4 °C to eliminate any unsolubilized material. The soluble fraction was incubated with the 1D4-Sepharose beads for 3 h, and the purified protein was eluted in either DM buffer or bicelle buffer containing 100 μM 1D4 9-mer peptide. All the procedures were performed in the dark on ice.

Purification of WT and G90V and N55K Mutants. WT opsin and G90V and N55K mutants were constructed on a synthetic bovine opsin gene in the pMT4 vector.[33] The WT and the G90V and N55K opsin mutants were transiently expressed in COS-1 cells by chemical transfection using PEI reagent as previously described.[34,35] After 48 h, the cells were harvested and regenerated with 10 μM 9-*cis*-retinal in solvent buffer via overnight incubation. Then the intact cells were solubilized in solvent buffer with 1% (w/v) DM containing 100

DOI: 10.1021/acs.biochem.5b00435
Biochemistry 2015, 54, 4795−4804

μM PMSF and protease inhibitors, followed by ultracentrifugation for 30 min in an Optima LE-80K Ultracentrifuge (Beckman Coulter) at 30000 rpm (50 Ti rotor). The supernatants were used for immunoaffinity chromatography purification with Sepharose coupled to the rho-1D4 antibody. The pigments were eluted, 3 h after incubation, with 100 μM 1D4 9-mer peptide in DM buffer or bicelle buffer. All the procedures were performed in the dark on ice. The samples in DM buffer and bicelle buffer were stored on ice and used within 36 h.

UV−Visible Absorption and Fluorescence Spectroscopies. UV−vis spectra were recorded with a Cary 100Bio spectrophotometer (Varian), equipped with water-jacketed cuvette holders connected to a circulating water bath. The temperature was controlled by a Peltier accessory connected to the spectrophotometer. All spectra were recorded in the range of 250−650 nm with a bandwidth of 2 nm, a response time of 0.1 s, and a scan speed of 300 nm/min. The spectral ratio is defined as the absorbance at 280 nm divided by the absorbance at the visible λ_{max} value to measure the pigment yield and the chromophore stability after purification. These samples were used for photobleaching, thermal bleaching, chromophore regeneration, MetaII decay, and chromophore entry experiments.

All fluorescence assays were performed by using a Photon Technologies QM-1 steady-state fluorescence spectrophotometer (PTI Technologies, Birmingham, NJ). The sample temperature was controlled with a TLC 50 Peltier accessory (Quantum Northwest, Liberty Lake, WA) connected to a hybrid liquid coolant system (Reserator XT, Zalman, Garden Grove, CA). Trp fluorescence was monitored over time. All fluorescence scans were conducted by exciting the samples for 2 s at 295 nm with a slit of 0.5 nm and blocking the excitation beam for 28 s with a beam shutter to avoid photobleaching of the sample. Trp emission was monitored at 330 nm with a slit of 10 nm.

Western Blot of WT and Mutants in the DM Detergent and in Bicelles. WT and G90V and N55K mutants were purified as described in either DM buffer or bicelle buffer. Then, 100 ng of purified protein was mixed with loading buffer and loaded onto a SDS−PAGE gel. After electrophoresis, the proteins were transferred to a nitrocellulose membrane and the protein bands visualized with the appropriate antibodies. The Rho 1D4 antibody dilution of 1:10000 was used for opsin detection, and the secondary antibody was goat anti-mouse HRP at a 1:5000 dilution. Both antibodies were dissolved in TBS with 0.1% (v/v) Tween buffer. Blots were developed using supersignal west pico chemiluminescent substrate (Thermo Fisher Scientific).

Thermal Bleaching Assay of the Purified Proteins. The thermal stability of Rho, WT, and its mutants was followed by UV−visible spectrophotometry. Pigment thermal bleaching rates were obtained, in the dark, by monitoring the decrease of absorbance at λ_{max} of the visible spectral band as a function of time at either 55 or 37 °C. Spectra were recorded every minute. Data points were obtained by using the equation $\Delta A = (A - A_f)/(A_0 - A_f)$, where A is the absorbance recorded at λ_{max}, A_f is the absorbance at the final time, and A_0 is the absorbance at time zero. The half-life time ($t_{1/2}$) for the process was determined by fitting the experimental data to single-exponential decay curves using Sigma Plot version 11.0 (Systat Software, Inc., Chicago, IL).

Regeneration of WT, G90V, and N55K. A 2.5-fold molar excess of 9-*cis*-retinal was added to the purified samples, in the dark, followed by illumination with a 150 W power source equipped with an optic fiber guide, using a >495 nm cutoff filter to avoid photobleaching of the free retinal. The samples were illuminated for 30 s at 20 °C, and spectra were recorded every minute until no further increase in $A_{\lambda max}$ was detected.

MetaII Decay Measurements. The MetaII active conformation decay process was followed in real time by fluorescence spectroscopy as previously described.[36] Briefly, 0.5 μM Rho in DM buffer, or bicelle buffer, was allowed to stabilize for 10 min at 20 °C in the fluorimeter, and the sample was subsequently illuminated for 30 s with a >495 nm cutoff filter. The increase in Trp fluorescence, due to release of retinal from MetaII (which parallels MetaII decay), was monitored, and after it had reached a plateau, 50 mM hydroxylamine hydrochloride (pH 7) was added to confirm complete retinal release. The $t_{1/2}$ values for the retinal release curves were determined by fitting the experimental data to single-exponential curves using Sigma Plot version 11.0 (Systat Software, Inc.).

Chromophore Re-entry after Photoactivation Measured by Fluorescence Spectroscopy. The retinal re-entry process was monitored in real time by means of fluorescence spectroscopy. A 2.5-fold retinal excess over pigment was added to the cuvette, after MetaII was completely decayed, and the changes in fluorescence intensity were recorded. The volume of the concentrated retinal stock added to the protein sample was 1% of the total sample volume.

RESULTS

UV−Vis Spectral Characterization of Purified WT and Mutants. WT and G90V and N55K mutants were purified from transfected COS-1 cells, and their UV−visible spectral properties, in either DM buffer (Figure 2) or bicelle buffer (Figure 3), were compared. A summary of the main spectral features of the DM buffer samples, including the λ_{max} value of the visible chromophoric band, the molar extinction coefficient (ε), and the spectral ratio ($A_{280}/A_{\lambda max}$), is shown in Table 1. The N55K mutant showed an $A_{280}/A_{\lambda max}$ ratio significantly higher than those of WT and the G90V mutant (Table 1), which implies a lower level of chromophore regeneration. Because 9-*cis*-retinal, and not 11-*cis*-retinal, was used for the regeneration of the recombinant proteins, the WT and the G90V and N55K mutants showed visible absorbance bands at 486, 480, and 480 nm, respectively. Upon illumination, G90V and N55K mutants showed incomplete conversion of the visible band to the 380 nm absorbing species, with ∼25% remaining absorbance at this wavelength indicating partial trapping of a photointermediate with a protonated SB linkage (Figure 2).[21,30] WT and G90V showed similar behavior upon illumination in bicelle buffer and DM buffer. In the case of N55K in bicelles, this mutant showed an altered photobleaching pattern, and additional illumination time was required to shift most of the visible band to 380 nm (Figure 3).

DMPC/DHPC Stabilization of ROS Rho. DMPC/DHPC bicelles were previously used to increase the thermal stability of purified Rho obtained from ROS membranes.[20,26,37] Here, ROS Rho, solubilized in DM (Rho_{DM}), was purified and used merely as a standard control. In this case, Rho was used to confirm the effectiveness of DMPC/DHPC bicelles in maintaining protein stability. The decay of the visible band (500 nm) was followed for Rho_{DM} and Rho in bicelles ($Rho_{bicelles}$) at 55 °C (Figure 4),

DOI: 10.1021/acs.biochem.5b00435
Biochemistry 2015, 54, 4795−4804

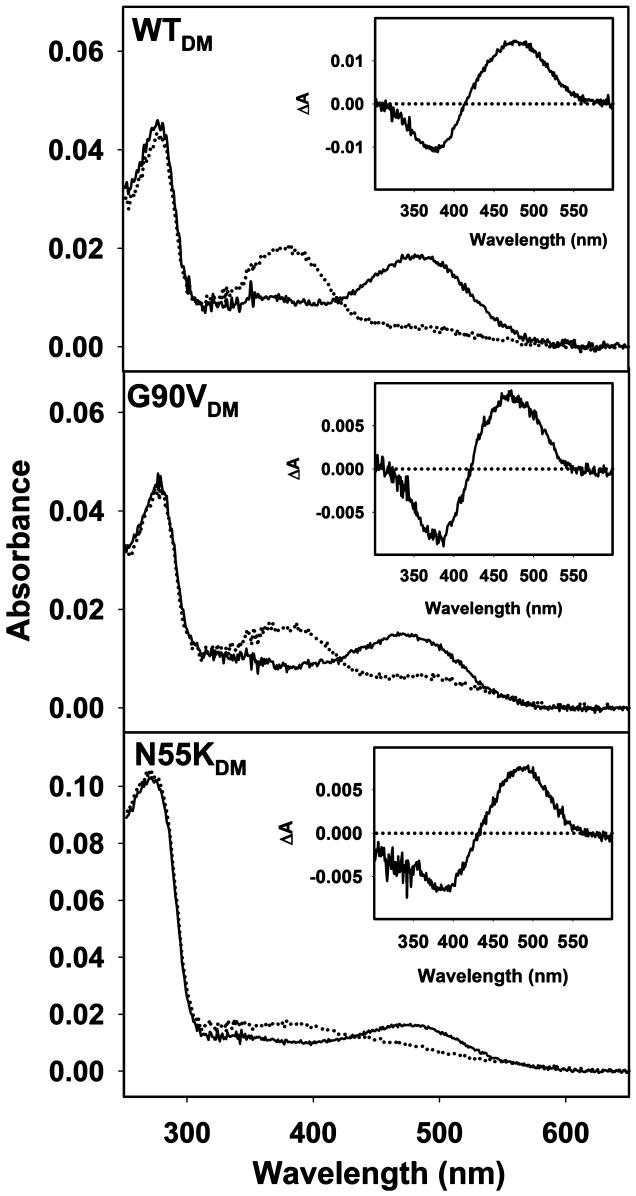

Figure 2. UV−vis characterization of WT, N55K, and G90V in DM buffer. WT, G90V, and N55K were immunopurified in DM buffer with 0.05% DM. The spectra were measured at 20 °C. Illumination was conducted for 30 s with a 150 W power source equipped with an optic fiber guide using a >495 nm cutoff filter to avoid photobleaching of the free retinal: (—) dark state and (···) photobleached state. The inset shows the difference spectrum (dark minus light).

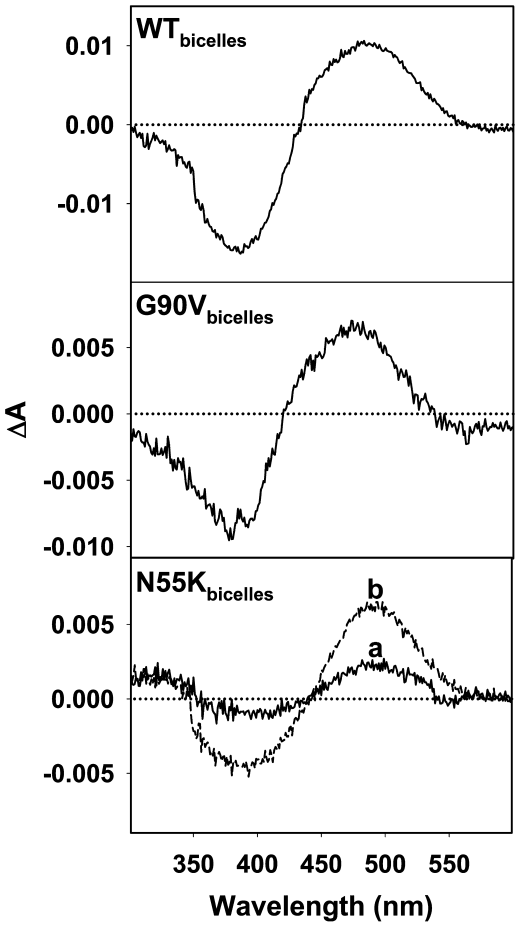

Figure 3. UV−vis difference spectra of WT, N55K, and G90V (dark minus light). WT, G90V, and N55K were purified in bicelle buffer. The spectra were measured at 20 °C. Illumination was conducted for 30 s with a 150 W power source equipped with an optic fiber guide using a >495 nm cutoff filter to avoid photobleaching of the free retinal. Notably, N55K$_{bicelles}$ showed only 20% photobleaching (a), and illumination for a further 30 s caused further A_{max} decay (b).

Table 1. Spectroscopic Properties of WT and RP Mutants Purified in DM Buffer

opsin	λ_{max} [a] (nm)	ε [b] (×10^3 M^{-1} cm^{-1})	$A_{280}/A_{\lambda max}$ [c]
WT	486 ± 3	43.2 ± 0.1	2.4 ± 0.1
G90V	480 ± 3	34.1 ± 0.5	3.0 ± 0.3
N55K	480 ± 2	35.5 ± 0.3	5.1 ± 1.6

[a]Mean values of the visible λ_{max} of WT and RP mutants G90V and N55K in DM buffer. [b]Each ε value was calculated with the equation $\varepsilon = (A/A_{Rho})(A_{440Rho}/A_{440})\varepsilon_{Rho}$, where A is the absorbance at the λ_{max} value, A_{440} is the absorbance at 440 nm after acid denaturation, and ε_{Rho} is the molar extinction of Rho (42.7 × 10^3 M^{-1} cm^{-1}).[21] [c]The $A_{280}/A_{\lambda max}$ ratio reflects the extent of chromophore regeneration. All values were determined from three independent experiments.

and the $t_{1/2}$ values for the process were determined. $t_{1/2}$ for Rho$_{bicelles}$ at 55 °C (41.2 ± 2.5 min) was ∼9-fold larger than $t_{1/2}$ for Rho$_{DM}$ (4.7 ± 0.4 min), indicating that DMPC/DHPC bicelles remarkably increase the thermal stability of Rho in comparison to that of the detergent-solubilized samples, in agreement with previous reports.[21,26]

Western Blot of WT and G90V and N55K Mutants in DM Buffer and Bicelle Buffer. Purified proteins were electrophoretically characterized by means of Western blot analysis (Figure 5). WT$_{bicelles}$ showed mobility bands higher than those of WT$_{DM}$, and this could be tentatively assigned to oligomeric species of Rho (dimers and higher-order oligomers), although the contribution of protein aggregation cannot be ruled out. G90V showed a prominent characteristic 27 kDa band that has been attributed to a truncated form of Rho. This band was detected both in DM and in bicelles. In the case of the N55K mutant, N55K$_{bicelles}$ showed a less intense 27 kDa band and an apparent increase in the high-molecular mass species band when compared to the N55K$_{DM}$ pattern.

Thermal Stability of WT, G90V, and N55K in DM and in DMPC/DHPC Bicelles. WT, G90V, and N55K were eluted in either DM buffer or bicelle buffer, and their thermal stability was determined at 37 °C (Figure 6a). A higher temperature, 55

DOI: 10.1021/acs.biochem.5b00435
Biochemistry 2015, 54, 4795−4804

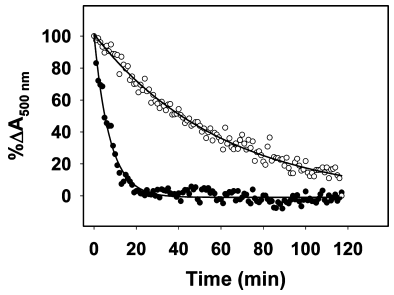

Figure 4. DMPC/DHPC stabilization of Rho from ROS. Thermal stability of Rho from ROS in either DM or bicelles at 55 °C. Purified Rho was dissolved in either DM buffer [Rho_{DM} (●)] or in bicelle buffer [$Rho_{bicelles}$ (○)]. Spectra were recorded at 55 °C, and normalized absorbance values at the A_{max} were plotted over time. Spectra were recorded every minute. At the end of the thermal decay, 50 mM hydroxylamine (pH 7.0) was added to confirm complete decay. Curves were fit to an exponential decay function.

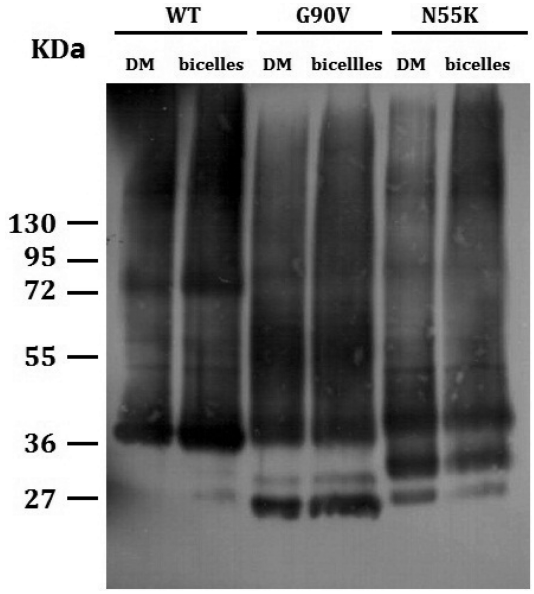

Figure 5. Western blot of WT, G90V, and N55K in either the DM detergent or bicelle conditions. WT, G90V, and N55K were purified from COS-1 cells either in DM buffer or in bicelle buffer. The same amount of protein was loaded onto a SDS−PAGE gel, subjected to electrophoresis, and subsequently transferred to a nitrocellulose membrane for detection. $WT_{bicelles}$ and $N55K_{bicelles}$ showed more higher-molecular weight species than WT_{DM} and $N55K_{DM}$. The two mutants showed clear bands below the main opsin band that could correspond to truncated Rho or to nonglyscosylated species.

°C, was chosen in previous studies, but the decay process was too fast at this temperature for the $t_{1/2}$ to be determined. At 37 °C, $G90V_{bicelles}$ and $N55K_{bicelles}$ showed enhanced thermal stability when compared to those of the DM-solubilized samples. The thermal decay process involves protein conformational changes, retinal isomerization, and eventually hydrolysis of SB and chromophore release.[20,38,39] We find that $t_{1/2}$ values of $G90V_{bicelles}$ and $N55K_{bicelles}$ increase 3- and 4-fold, respectively, compared to those of the detergent-solubilized samples (Figure 6a and Table 2).

Chromophore Regeneration Measurements. The effect of DMPC/DHPC bicelles on pigment regeneration after photobleaching was analyzed for the purified proteins. The maximal extent of regeneration and the regeneration rate were

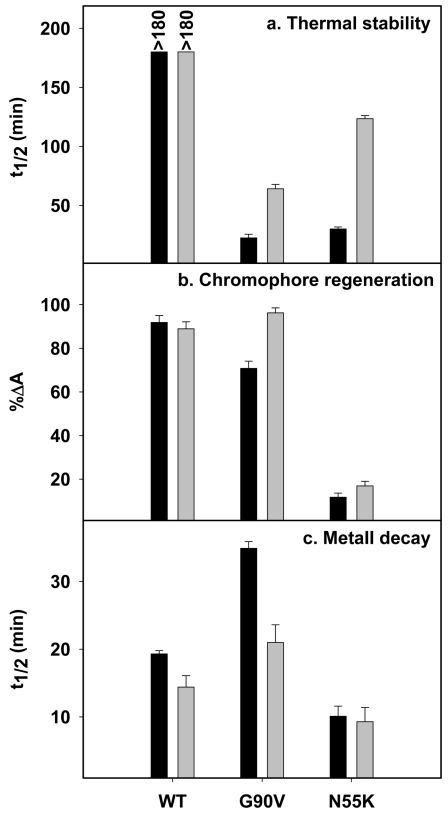

Figure 6. Conformational properties of WT and RP mutants from thermal stability, chromophore regeneration, and MetaII decay experiments. WT, G90V, and N55K were purified in DM buffer (black bar) and bicelle buffer (gray bar). (a) $t_{1/2}$ values of WT, G90V, and N55K mutants from thermal bleaching experiments at 37 °C. (b) Chromophore regeneration percentage of WT, G90V, and N55K mutants. (c) $t_{1/2}$ values of WT, G90V, and N55K in MetaII decay experiments. The numerical values for the measured times are listed in Table 2. The mean and error bars of three independent measurements are represented.

the main factors analyzed (Figure 6b). The extent of WT regeneration was similar for $WT_{bicelles}$ and WT_{DM}. However, $G90V_{bicelles}$ showed 20% more chromophore regeneration than $G90V_{DM}$. Remarkably, N55K exhibited a special behavior because, upon illumination, only 30−40% appeared to be photobleached and the added chromophore did not significantly improve N55K regeneration (Figure 6b and Table 2).

Meta II Decay Measurements. MetaII stability was studied by fluorescence spectroscopy, which measures retinal release upon sample illumination.[36] Overall, the retinal release process was faster in bicelles than in DM samples. Under both conditions, $t_{1/2}$ values for retinal release followed the order G90V ≫ WT > N55K, G90V being the slowest (Figures 6c and 7 and Table 2). This behavior may be tentatively associated with the clinical phenotypes caused by these mutations. In all cases, bicelles have decreased the $t_{1/2}$ of the retinal release process for WT (25.4%), G90V (39.8%), and N55K (7.9%) compared with the same process in DM buffer (Figures 6c and 7 and Table 2). Hydroxylamine was added to confirm complete retinal release. No changes were detected for the samples in DM buffer (Figure 7A), but in the bicelle environment, both WT and G90V showed a slight additional increase in Trp fluorescence emission, which suggested additional release of retinal from the binding pocket (Figure 7B). N55K did not

DOI: 10.1021/acs.biochem.5b00435
Biochemistry 2015, 54, 4795−4804

Table 2. Molecular Properties of WT and RP Mutants from Thermal Stability, Chromophore Regeneration, and MetaII Decay Experiments in DM and Bicelles

	buffer	WT	G90V	N55K
thermal bleaching[a]	DM	>180 min	22.5 ± 3.1 min	30.1 ± 1.7 min
	bicelles	>180 min	64.1 ± 3.7 min	123.5 ± 2.6 min
regeneration[b]	DM	91.8 ± 3.2%	70.8 ± 3.3%	11.7 ± 1.9%
	bicelles	88.9 ± 3.2%	96.2 ± 2.3%	16.9 ± 2.1%
MetaII decay[c]	DM	19.3 ± 0.5 min	34.9 ± 1.0 min	10.1 ± 1.5 min
	bicelles	14.4 ± 1.7 min	21.0 ± 2.6 min	9.3 ± 2.1 min

[a] $t_{1/2}$ of WT, G90V, and N55K in thermal bleaching experiments. Thermal decay experiments were conducted at 37 °C. At the end of the thermal decay, 50 mM hydroxylamine (pH 7.0) was added to confirm complete decay. Curves were fit to an exponential decay function. [b] Regeneration percentage of WT, G90V, and N55K. Retinal was added before illumination, and spectra were recorded every minute after illuminating the samples for 30 s. These experiments were conducted at 20 °C. [c] Retinal release $t_{1/2}$ of WT, G90V, and N55K. Samples were stabilized for 10 min in the dark and subsequently illuminated for 30 s (λ > 495 nm). The fluorescence increase was measured until the signal reached a plateau; 50 mM hydroxylamine (pH 7.0) was added to confirm complete retinal release. The $t_{1/2}$ of the retinal release was determined from the exponential curves.

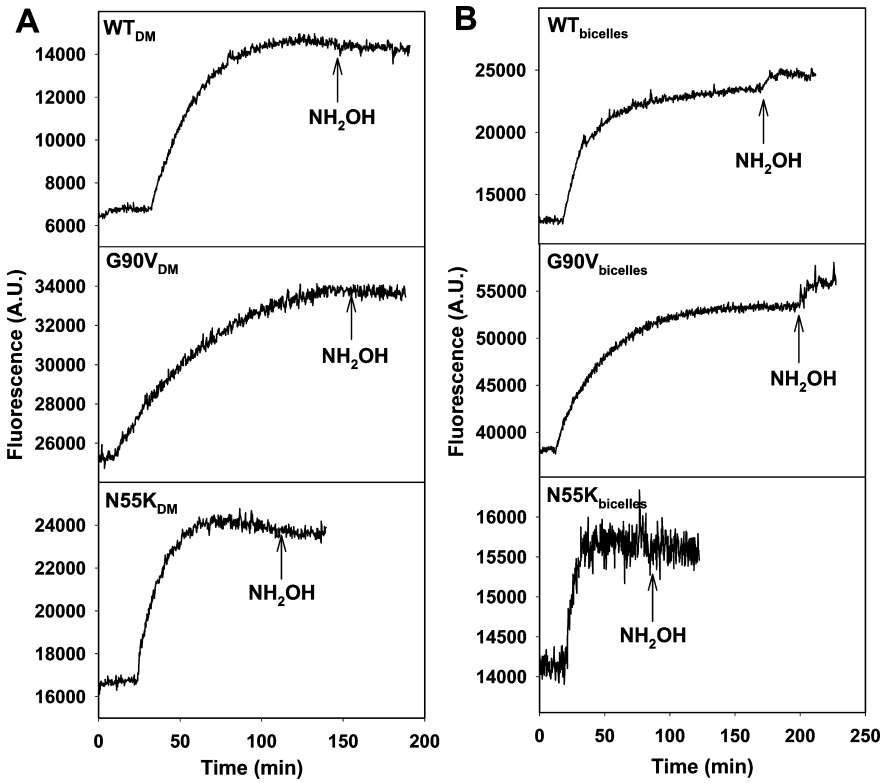

Figure 7. MetaII decay for WT, G90V, and N55K. WT, G90V, and N55K were purified in either DM buffer (A) or bicelle buffer (B). The samples were illuminated for 30 s (>495 nm) after the dark-state fluorescence intensity was stabilized. After MetaII decay and once the fluorescence intensity reached a plateau, 50 mM hydroxylamine (pH 7.0) was added to confirm complete retinal release.

show any increases and remained stable in both DM and the bicelle environment (Figure 7A,B). This result is in contrast to that obtained in a previous study in which N55K was in PBS (pH 7.4) containing 0.05% DM.[30] In that case, hydroxylamine did cause an increase in the fluorescence signal, which points to a strong effect of buffer in the spectrofluorimetric measurements.

Opsin Conformational Stability after Retinal Release. WT, G90V, and N55K, in DM buffer or bicelle buffer, were analyzed by fluorescence spectroscopy to follow the potential ability of 9-*cis*-retinal to enter the opsin pocket after complete MetaII decay. Thus, 2.5-fold exogenous 9-*cis*-retinal was added, after complete retinal release (plateau in the fluorescence curve), to test whether this ligand could enter the binding pocket. WT_{DM} showed only a minor reduction in Trp fluorescence, upon retinal addition, suggesting that the retinal ligand could not significantly enter its binding pocket (Figure 8A). A clear decrease in fluorescence could be detected in the case of $WT_{bicelles}$, indicating that the exogenous chromophore could enter the binding pocket thus quenching Trp fluorescence (Figure 8B). The structurally unstable mutants G90V and N55K showed a clear distinct behavior. Exogenous addition of 9-*cis*-retinal resulted in an important decrease in the magnitude of the fluorescence signal for $G90V_{DM}$ and a further decrease for $G90V_{bicelles}$ (Figure 8). However, no change was observed for N55K either in DM or in bicelles, suggesting that this mutation impaired the entry of retinal into the binding pocket. Similar results were obtained when the experiments were conducted by using 11-*cis*-retinal (data not shown).

DOI: 10.1021/acs.biochem.5b00435
Biochemistry 2015, 54, 4795−4804

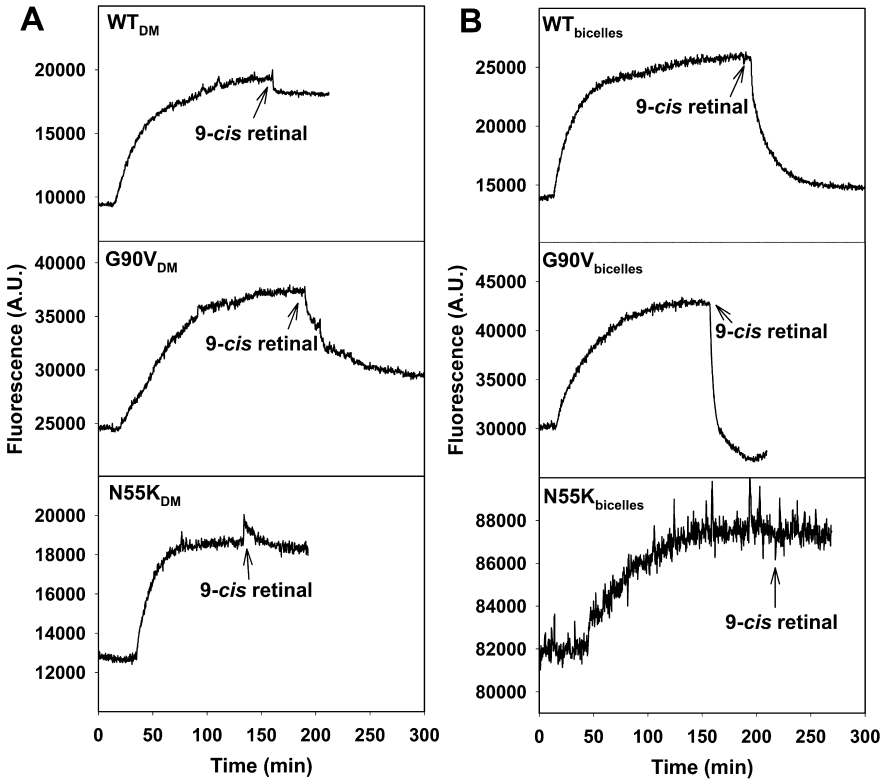

Figure 8. Retinal entry in photoactivated opsin. After the fluorescence intensity reached a plateau, from the MetaII decay experiment, for WT, N55K, and G90V pigments purified either in DM buffer (A) or in bicelle buffer (B), retinal was added (2.5-fold excess of exogenous retinal to the concentration of pigment) and mixed well to detect entry of retinal into the binding pocket. $WT_{bicelles}$ and $G90V_{bicelles}$ showed a fluorescence decrease greater than that of the DM samples, whereas $N55K_{bicelles}$ did not show any change upon retinal addition.

DISCUSSION

Rho mutants (both synthetic and naturally occurring) have been widely studied to unravel the molecular mechanisms of GPCR activation and signaling, and the molecular mechanisms of RP retinal degenerative disease.[16,40,41] Some of these mutations can cause structural instability and misfolding.[42] The stability of visual photoreceptors, and other GPCRs, has been extensively studied, and several experimental factors, like temperature, pH, salts, detergents, and lipids, have been shown to affect the stability and function of these receptors.[8,22,28,43−46] In spite of this, only limited information is available concerning the molecular causes of the structural instability of mutations in Rho associated with RP. In clear contrast with detergents, lipid bilayers have been shown to increase the stability and facilitate the folding, assembly, and function of membrane proteins.[17,27,28] Here, we purified the newly reported unstable RP mutants, G90V and N55K, in DMPC/DHPC bicelles. This bicelle system has been proposed to support the folding and thermal stability of Rho and opsin.[26] Such a system has been used in solid-state nuclear magnetic resonance (NMR) studies of membrane-associated molecules, and its use extended to non-NMR-based biophysical studies of transmembrane proteins.[27,47−49]

The structural arrangement of Rho in DM and in bicelles shows important differences. DM would form micelles to embed Rho, whereas DMPC and DHPC shaped bicelles that could better mimic the membrane environment (Figure 1). The UV−visible characterization of WT, N55K, and G90V in DM detergent was conducted with 9-*cis*-retinal-regenerated samples. The 9-*cis* isomer was used because it has been previously shown that this isomer can improve chromophore regeneration of Rho mutants.[21] The visible bands of the WT and the mutants where blue-shifted, with regard to those of the 11-*cis*-retinal-containing samples, because of the specific interaction of 9-*cis*-retinal with the amino acids in the binding pocket. The N55K mutant showed an $A_{280}/A_{\lambda max}$ higher than that of WT in DM buffer, which could imply lower chromophore stability during the purification process, as previously described.[30] The two mutations studied, G90V and N55K, showed abnormal photobleaching behavior, in DM buffer, with incomplete conversion of the visible band upon illumination (Figure 2). In bicelle buffer, G90V showed WT-like behavior but N55K showed an altered photobleaching pattern (Figure 3), indicating that bicelles stabilized either its dark state or a photointermediate conformation. Electrophoretic analysis of the purified mutant proteins revealed differences in the intensities of bands that would correspond to dimeric (or higher-order oligomeric) conformations that appeared to be favored in bicelles. Interestingly, G90V and N55K mutants showed the presence of lower bands in the 25−30 kDa range, particularly a 27 kDa band that has been attributed to a truncated form of opsin.[50,51] This behavior suggests that the mutants may have increased susceptibility to protein truncation that may be associated with a decreased conformational stability and may be linked to the molecular phenotype underlying the pathological nature of the mutations.

The thermal stability for the mutants at 37 °C has been clearly improved in the bicelle system. In particular, $N55K_{bicelles}$ showed a 4-fold increase in thermal stability compared with that of $N55K_{DM}$, at this temperature, meaning that bicelles provide conformational stability and protect the SB linkage from hydrolysis.[39] Chromophore regeneration represents also

DOI: 10.1021/acs.biochem.5b00435
Biochemistry 2015, 54, 4795−4804

an important index that reflects the structural stability of Rho mutants. $G90V_{bicelles}$ showed a 20% chromophore regeneration increase compared to that of $G90V_{DM}$. From the fluorescence experiments, this mutant also showed an increased level of entry of retinal into the binding pocket a long time after illumination, in the bicelle sample, suggesting that lipids play a role in the regeneration process by helping stabilize its optimal ligand binding conformation. In contrast, N55K did not show any improvement in chromophore regeneration, which is consistent with the mutation impairing retinal release due to specific interactions at the transmembrane domain of the receptor. This trend would be maintained in the case of this mutant in the bicelle environment.

In the MetaII decay experiment, after the sample was illuminated and the active MetaII conformation decayed, addition of subsequent hydroxylamine resulted in an additional fluorescence increase for $WT_{bicelles}$ and $G90D_{bicelles}$. This suggests that bicelles can increase the residence time of all-*trans*-retinal in the binding pocket, thus extending the available time for G-protein activation.[6] On the other hand, N55K did not show any difference, after hydroxylamine addition, either in DM detergent or in bicelle buffer. We have previously reported that PBS with 0.05% DM could increase the magnitude of the fluorescence signal.[30] Thus, the buffer conditions clearly influence the fluorescence assay.

The fluorescence decrease upon retinal addition, after complete MetaII decay (Figure 8), would indicate that retinal can enter the retinal binding pocket, although this does not demonstrate covalent binding to the opsin moiety. This suggests that bicelles help to maintain a stable opsin structure a long time after complete retinal release, thus favoring binding of retinal to the protein. Interestingly, N55K did not show any decrease, either in DM or in bicelles, and this is a differential effect only seen for this mutant that may be associated with the sector RP phenotype restricted mostly to the inferior quadrants of the retina.[19] This unique N55K behavior may provide new clues that would guide us in deciphering the molecular mechanism of sector RP. We have previously associated this mechanism with different responses to light by this mutant.[30]

Both mutations studied, N55K and G90D, correspond to amino acids that are facing the protein interior and are mainly involved in helix−helix interactions. Thus, residues at positions 55 and 90 are not facing the lipid or involved in monomer−monomer interactions (Figure 9). Furthermore, the residues do not appear to significantly alter their orientation (or interactions) in the activated state of the receptor.[12]

In the case of N55K, this mutation is located in transmembrane helix 1 in a region closer to the cytoplasmic side of the protein where the G-protein activation process takes place. Three highly conserved residues, throughout the GPCR superfamily, toward the cytoplasmic side of the receptor, N55 (98%), D83 (92%), and N302 (77%), define a region with intimate contact among TMs 1, 2, and 7, which involves also various highly conserved water molecules. In the N55K substitution, the Lys side chain would interfere with these contacts and could form a salt bridge with D83 (Figure 9). The G90V mutation affects an amino acid, at transmembrane helix 2, which is located toward the intradiscal domain of the protein that plays a structural role in the folding of the receptor and in the retinal binding process. The reported G90V mutant behavior suggests an important role for a functional water molecule present in the vicinity of E113 and the SB in the dark-state crystal structure of Rho.[21] This water molecule binds to both the carbonyl backbone and one of the carboxyl oxygens of E113. The lack of a side chain at G90 gives an empty volume that is filled with such a water molecule, whereas the hydrophobic chain in G90V would either not allow the water molecule to be accommodated or result in a lower affinity. The lack of the water molecule would alter the metarhodopsin I to MetaII transition energy landscape and would also decrease dark-state stability, in agreement with the results presented here.[21]

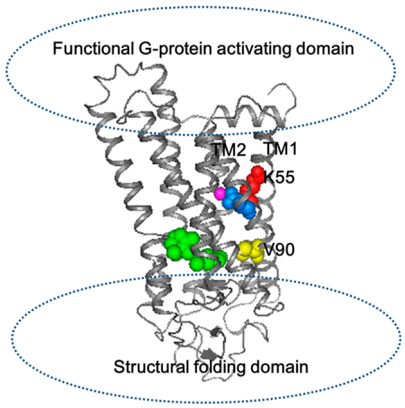

Figure 9. Structural model of Rho showing the sites of mutations. Lys at position 55 (red) and Val at position 90 (yellow) are shown together with other relevant molecules, like retinal (green), Asp83 (blue), and water (magenta). Although the two mutations are located in the transmembrane domain of the protein, Lys55 is closer to the cytoplasmic domain where the G-protein activating function of the receptor takes place, whereas Val90 is closer to the retinal binding site and the intradiscal domain, a region of the protein that governs its folding and stability. The Rho dark-state crystal structure (Protein Data Bank entry 3C9L) was used, and the image was created using PyMol (Schrodinger, LLC, The PyMOL Molecular Graphics System, version 1.5).

The influence of membrane morphology and composition on receptor structure and function is undoubtedly a key factor to take into account when analyzing the effect of mutations, particularly those associated with disease. We have reported a significant effect of DMPC/DHPC bicelles in the stabilization of Rho mutants associated with RP retinal disease. In the case of G90V, a significant increase in the chromophore thermal stability and regeneration was observed, which is likely due to the stabilizing effect of the lipid bicelles on the opsin conformation of the mutant. The other studied mutant, N55K, associated with the peculiar sector RP phenotype,[30] shows also improved thermal stability but no improvement in its retinal regeneration ability. This would be due to the specificity imposed by the Lys introduced into the transmembrane domain of the photoreceptor protein[30] that would entrap the retinal molecule, impairing efficient retinal regeneration after photobleaching. Overall, our results underscore the importance of the topological arrangement of lipids in stabilizing critical interhelical interactions and promoting favorable helical packing forces that would be absent in detergent-solubilized samples. Further in-depth studies of the structural and energetic features of the lipid−protein interactions are needed to decipher the structural basis of the differential stability seen for Rho mutations. This knowledge is important to provide functionally relevant structural information that can be useful in the development of targeted therapies toward retinal degenerative diseases.

DOI: 10.1021/acs.biochem.5b00435
Biochemistry 2015, 54, 4795−4804

AUTHOR INFORMATION

Corresponding Author

*Grup de Biotecnologia Molecular i Industrial, Centre de Biotecnologia Molecular, Departament d'Enginyeria Química, Universitat Politècnica de Catalunya, Rambla de Sant Nebridi 22, 08222 Terrassa, Spain. Telephone: +34 937398568. Fax: +34 937398225. E-mail: pere.garriga@upc.edu.

Funding

This work was supported by grants from Ministerio de Ciencia e Innovación (Spain) (SAF2011-30216-C02-01), Grups de Recerca Consolidats from Generalitat de Catalunya (2009 SGR 1402), and Fundación Areces (to P.G.) and by a CIG grant from the EUROPEAN Commission (to E.R.). X.D. is the recipient of a predoctoral scholarship from the Chinese Scholarship Council (CSC). M.G.H.-H. is the recipient of a predoctoral scholarship from CONACYT Mexico.

Notes

The authors declare no competing financial interest.

†M.G.H.-H. on leave from: Unidad de Biotecnología, Campo Experimental Bajío (INIFAP), Km 6.5 Carretera Celaya-San Miguel Allende s/n, México, CP 38110.

ACKNOWLEDGMENTS

We thank Sundaramoorthy Srinivasan, Miguel A. Fernández Sampedro, and Margarita Morillo for helpful discussions.

ABBREVIATIONS

GPCRs, G-protein-coupled receptors; RP, retinitis pigmentosa; sector RP, sector retinitis pigmentosa; ROS, rod outer segment; Rho, rhodopsin; WT, wild type; DMPC, 1,2-dimyristoyl-*sn*-glycero-3-phosphatidylcholine; DHPC, 1,2-dihexanoyl-*sn*-glycero-3-phosphocholine; DM, *n*-dodecyl D-maltoside; SB, Schiff base; BTP, bis-tris-propane; SDS−PAGE, sodium dodecyl sulfate−polyacrylamide gel electrophoresis; MetaII, metarhodopsin II.

REFERENCES

(1) Fredriksson, R., Lagerstrom, M. C., Lundin, L.-G., and Schioth, H. B. (2003) The G-protein-coupled receptors in the human genome form five main families. Phylogenetic analysis, paralogon groups, and fingerprints. *Mol. Pharmacol. 63*, 1256−1272.

(2) Tesmer, J. J. G. (2010) The quest to understand heterotrimeric G protein signaling. *Nat. Struct. Mol. Biol. 17*, 650−652.

(3) Hiller, C., Kuhhorn, J., and Gmeiner, P. (2013) Class A G-protein-coupled receptor (GPCR) dimers and bivalent ligands. *J. Med. Chem. 56*, 6542−6559.

(4) Rosenbaum, D. M., Rasmussen, S. G. F., and Kobilka, B. K. (2009) The structure and function of G-protein-coupled receptors. *Nature 459*, 356−363.

(5) Venkatakrishnan, A. J., Deupi, X., Lebon, G., Tate, C. G., Schertler, G. F., and Babu, M. M. (2013) Molecular signatures of G-protein-coupled receptors. *Nature 494*, 185−194.

(6) Wang, Y., Botelho, A. V., Martinez, G. V., and Brown, M. F. (2002) Electrostatic properties of membrane lipids coupled to metarhodopsin II formation in visual transduction. *J. Am. Chem. Soc. 124*, 7690−7701.

(7) Gibson, N. J., and Brown, M. F. (1991) Membrane lipid influences on the energetics of the metarhodopsin I and metarhodopsin II conformational states of rhodopsin probed by flash photolysis. *Photochem. Photobiol. 54*, 985−992.

(8) Huber, T., Rajamoorthi, K., Kurze, V. F., Beyer, K., and Brown, M. F. (2002) Structure of docosahexaenoic acid-containing phospholipid bilayers as studied by (2)H NMR and molecular dynamics simulations. *J. Am. Chem. Soc. 124*, 298−309.

(9) Boesze-Battaglia, K., and Schimmel, R. (1997) Cell membrane lipid composition and distribution: implications for cell function and lessons learned from photoreceptors and platelets. *J. Exp. Biol. 200*, 2927−2936.

(10) Hernandez-Rodriguez, E. W., Sanchez-Garcia, E., Crespo-Otero, R., Montero-Alejo, A. L., Montero, L. A., and Thiel, W. (2012) Understanding rhodopsin mutations linked to the retinitis pigmentosa disease: a QM/MM and DFT/MRCI study. *J. Phys. Chem. B 116*, 1060−1076.

(11) Lamb, T. D., and Pugh, E. N. J. (2006) Phototransduction, dark adaptation, and rhodopsin regeneration the proctor lecture. *Invest. Ophthalmol. Visual Sci. 47*, 5137−5152.

(12) Hofmann, K. P., Scheerer, P., Hildebrand, P. W., Choe, H.-W., Park, J. H., Heck, M., and Ernst, O. P. (2009) A G protein-coupled receptor at work: the rhodopsin model. *Trends Biochem. Sci. 34*, 540−552.

(13) Yau, K.-W., and Hardie, R. C. (2009) Phototransduction motifs and variations. *Cell 139*, 246−264.

(14) Daiger, S. P., Sullivan, L. S., and Bowne, S. J. (2013) Genes and mutations causing retinitis pigmentosa. *Clin. Genet. 84*, 132−141.

(15) Rayapudi, S., Schwartz, S. G., Wang, X., and Chavis, P. (2013) Vitamin A and fish oils for retinitis pigmentosa. *Cochrane database of systematic reviews 12*, CD008428.

(16) Krebs, M. P., Holden, D. C., Joshi, P., Clark, C. L., 3rd, Lee, A. H., and Kaushal, S. (2010) Molecular mechanisms of rhodopsin retinitis pigmentosa and the efficacy of pharmacological rescue. *J. Mol. Biol. 395*, 1063−1078.

(17) Saliba, R. S., Munro, P. M. G., Luthert, P. J., and Cheetham, M. E. (2002) The cellular fate of mutant rhodopsin: quality control, degradation and aggresome formation. *Journal of cell science 115*, 2907−2918.

(18) Ulloa-Aguirre, A., Zarinan, T., Dias, J. A., and Conn, P. M. (2014) Mutations in G protein-coupled receptors that impact receptor trafficking and reproductive function. *Mol. Cell. Endocrinol. 382*, 411−423.

(19) Van Woerkom, C., and Ferrucci, S. (2005) Sector retinitis pigmentosa. *Optometry (St. Louis, Mo.) 76*, 309−317.

(20) Ramon, E., Marron, J., del Valle, L., Bosch, L., Andres, A., Manyosa, J., and Garriga, P. (2003) Effect of dodecyl maltoside detergent on rhodopsin stability and function. *Vision Res. 43*, 3055−3061.

(21) Toledo, D., Ramon, E., Aguila, M., Cordomi, A., Perez, J. J., Mendes, H. F., Cheetham, M. E., and Garriga, P. (2011) Molecular mechanisms of disease for mutations at Gly-90 in rhodopsin. *J. Biol. Chem. 286*, 39993−40001.

(22) Sanchez-Martin, M. J., Ramon, E., Torrent-Burgues, J., and Garriga, P. (2013) Improved conformational stability of the visual G protein-coupled receptor rhodopsin by specific interaction with docosahexaenoic acid phospholipid. *ChemBioChem 14*, 639−644.

(23) Tsukamoto, H., Szundi, I., Lewis, J. W., Farrens, D. L., and Kliger, D. S. (2011) Rhodopsin in nanodiscs has native membrane-like photointermediates. *Biochemistry 50*, 5086−5091.

(24) Reeves, P. J., Hwa, J., and Khorana, H. G. (1999) Structure and function in rhodopsin: kinetic studies of retinal binding to purified opsin mutants in defined phospholipid-detergent mixtures serve as probes of the retinal binding pocket. *Proc. Natl. Acad. Sci. U. S. A. 96*, 1927−1931.

(25) Serebryany, E., Zhu, G. A., and Yan, E. C. Y. (2012) Artificial membrane-like environments for in vitro studies of purified G-protein coupled receptors. *Biochim. Biophys. Acta, Biomembr. 1818*, 225−233.

(26) McKibbin, C., Farmer, N. A., Jeans, C., Reeves, P. J., Khorana, H. G., Wallace, B. A., Edwards, P. C., Villa, C., and Booth, P. J. (2007) Opsin stability and folding: modulation by phospholipid bicelles. *J. Mol. Biol. 374*, 1319−1332.

(27) Sanders, C. R., and Prosser, R. S. (1998) Bicelles: a model membrane system for all seasons? *Structure (Oxford, U. K.) 6*, 1227−1234.

DOI: 10.1021/acs.biochem.5b00435
Biochemistry 2015, 54, 4795−4804

(28) Kaya, A. I., Thaker, T. M., Preininger, A. M., Iverson, T. M., and Hamm, H. E. (2011) Coupling efficiency of rhodopsin and transducin in bicelles. *Biochemistry 50*, 3193−3203.
(29) Neidhardt, J., Barthelmes, D., Farahmand, F., Fleischhauer, J. C., and Berger, W. (2006) Different amino acid substitutions at the same position in rhodopsin lead to distinct phenotypes. *Invest. Ophthalmol. Visual Sci. 47*, 1630−1635.
(30) Ramon, E., Cordomi, A., Aguila, M., Srinivasan, S., Dong, X., Moore, A. T., Webster, A. R., Cheetham, M. E., and Garriga, P. (2014) Differential light-induced responses in sectorial inherited retinal degeneration. *J. Biol. Chem. 289*, 35918−35928.
(31) Sekharan, S., and Morokuma, K. (2011) Why 11-cis-retinal? Why not 7-cis-, 9-cis-, or 13-cis-retinal in the eye? *J. Am. Chem. Soc. 133*, 19052−19055.
(32) Srinivasan, S., Ramon, E., Cordomi, A., and Garriga, P. (2014) Binding specificity of retinal analogs to photoactivated visual pigments suggest mechanism for fine-tuning GPCR-ligand interactions. *Chem. Biol. 21*, 369−378.
(33) Oprian, D. D., Molday, R. S., Kaufman, R. J., and Khorana, H. G. (1987) Expression of a synthetic bovine rhodopsin gene in monkey kidney cells. *Proc. Natl. Acad. Sci. U. S. A. 84*, 8874−8878.
(34) Longo, P. A., Kavran, J. M., Kim, M.-S., and Leahy, D. J. (2013) Transient mammalian cell transfection with polyethylenimine (PEI). *Methods Enzymol. 529*, 227−240.
(35) Hacker, D. L., Kiseljak, D., Rajendra, Y., Thurnheer, S., Baldi, L., and Wurm, F. M. (2013) Polyethyleneimine-based transient gene expression processes for suspension-adapted HEK-293E and CHO-DG44 cells. *Protein Expression Purif. 92*, 67−76.
(36) Farrens, D. L., and Khorana, H. G. (1995) Structure and function in rhodopsin. Measurement of the rate of metarhodopsin II decay by fluorescence spectroscopy. *J. Biol. Chem. 270*, 5073−5076.
(37) Jastrzebska, B., Debinski, A., Filipek, S., and Palczewski, K. (2011) Role of membrane integrity on G protein-coupled receptors: Rhodopsin stability and function. *Prog. Lipid Res. 50*, 267−277.
(38) Fotiadis, D., Liang, Y., Filipek, S., Saperstein, D. A., Engel, A., and Palczewski, K. (2003) Atomic-force microscopy: Rhodopsin dimers in native disc membranes. *Nature 421*, 127−128.
(39) Liu, J., Liu, M. Y., Nguyen, J. B., Bhagat, A., Mooney, V., and Yan, E. C. Y. (2009) *J. Am. Chem. Soc. 131*, 8750−8751.
(40) Golovleva, I., Bhattacharya, S., Wu, Z., Shaw, N., Yang, Y., Andrabi, K., West, K. A., Burstedt, M. S. I., Forsman, K., Holmgren, G., Sandgren, O., Noy, N., Qin, J., and Crabb, J. W. (2003) Disease-causing mutations in the cellular retinaldehyde binding protein tighten and abolish ligand interactions. *J. Biol. Chem. 278*, 12397−12402.
(41) Petrs-Silva, H., and Linden, R. (2014) Advances in gene therapy technologies to treat retinitis pigmentosa. *Clin. Ophthalmol. 8*, 127−136.
(42) Tzekov, R., Stein, L., and Kaushal, S. (2011) Protein misfolding and retinal degeneration. *Cold Spring Harbor Perspect. Biol. 3*, a007492.
(43) Rozin, R., Wand, A., Jung, K.-H., Ruhman, S., and Sheves, M. (2014) pH dependence of Anabaena sensory rhodopsin: retinal isomer composition, rate of dark adaptation, and photochemistry. *J. Phys. Chem. B 118*, 8995−9006.
(44) Parkes, J. H., Gibson, S. K., and Liebman, P. A. (1999) Temperature and pH dependence of the metarhodopsin I-metarhodopsin II equilibrium and the binding of metarhodopsin II to G protein in rod disk membranes. *Biochemistry 38*, 6862−6878.
(45) Alves, I. D., Salgado, G. F. J., Salamon, Z., Brown, M. F., Tollin, G., and Hruby, V. J. (2005) Phosphatidylethanolamine enhances rhodopsin photoactivation and transducin binding in a solid supported lipid bilayer as determined using plasmon-waveguide resonance spectroscopy. *Biophys. J. 88*, 198−210.
(46) Sato, K., Morizumi, T., Yamashita, T., and Shichida, Y. (2010) Direct observation of the pH-dependent equilibrium between metarhodopsins I and II and the pH-independent interaction of metarhodopsin II with transducin C-terminal peptide. *Biochemistry 49*, 736−741.
(47) Sanders, C. R., and Oxenoid, K. (2000) *Biochim. Biophys. Acta, Biomembr. 1508*, 129−145.
(48) Fernández, C., Hilty, C., Wider, G., and Wüthrich, K. (2002) Lipid-protein interactions in DHPC micelles containing the integral membrane protein OmpX investigated by NMR spectroscopy. *Proc. Natl. Acad. Sci. U. S. A. 99*, 13533−13537.
(49) Marcotte, I., and Auger, M. (2005) Bicelles as model membranes for solid-and solution-state NMR studies of membrane peptides and proteins. *Concepts Magn. Reson., Part A 24*, 17−35.
(50) Janz, J. M., Fay, J. F., and Farrens, D. L. (2003) Stability of dark state rhodopsin is mediated by a conserved ion pair in intradiscal loop E-2. *J. Biol. Chem. 278*, 16982−16991.
(51) Sung, C. H., Schneider, B. G., Agarwal, N., Papermaster, D. S., and Nathans, J. (1991) Functional heterogeneity of mutant rhodopsins responsible for autosomal dominant retinitis pigmentosa. *Proc. Natl. Acad. Sci. U. S. A. 88*, 8840−8844.

DOI: 10.1021/acs.biochem.5b00435
Biochemistry 2015, 54, 4795−4804